IX ECCOMAS Thematic Conference on Smart Structures and Materials
SMART 2019
A. Benjeddou, N. Mechbal and J.F. Deü (Eds)

INVESTIGATIONS ABOUT THE MODELLING OF ACOUSTIC PROPERTIES OF PERIODIC POROUS MATERIALS WITH THE SHIFT CELL APPROACH

D. MAGLIACANO[*†], M. OUISSE[*], S. DE ROSA[†], F. FRANCO[†] AND A. KHELIF[*]

[*]Univ. Bourgogne Franche-Comté // FEMTO-ST Institute // CNRS/UFC/ENSMM/UTBM
Department of Applied Mechanics // 25000 Besançon, FRANCE

[†]⌘ PASTA-Lab (Laboratory for Promoting experiences in Aeronautical STructures and Acoustics)
Department of Industrial Engineering - Aerospace Section
Università degli Studi di Napoli "Federico II"
Via Claudio 21, Edificio 11, 80125 Napoli, ITALY

Key words: vibroacoustics, periodic structure, shift cell, foam, inclusion

Abstract: The main advantage of designing sound packages with periodic arrangements is that they can provide a combination of absorption effects, resonance effects and wave interferences effects. This offers different applications in transportation (aeronautics, space, automotive, railway), energy and civil engineering sectors, where both weight and space, as well as vibroacoustic quality of performance and comfort, still remain as critical issues. The application of shift cell technique is presented and discussed for periodic porous media described with equivalent fluid models: it consists in a reformulation of classical Floquet-Bloch (F-B) conditions, whose major advantage stands in allowing the introduction of any frequency dependence of porous material behavior, through the resolution a quadratic eigenvalue problem, providing an efficient way to compute the dispersion curves of a porous material modelled as an equivalent fluid. The central part of this work shows the results, in terms of absorption coefficient and transmission loss curves, obtained through a numerical test campaign involving different melamine and polyurethane foams. The 48 test cases involve a cubic unit cell of porous material with a cylindrical inclusion. Furthermore, some absorption coefficient and transmission loss comparisons are shown, between a homogeneous unit cell and a unit cell with a perfectly rigid inclusion; the comparisons are carried out at fixed dimensions, then at fixed mass and then at fixed performance in the periodicity peak range. The results clearly point out the advantage of designing foam layer with periodic inclusion patterns in order to improve the performances in a specific range of frequencies, allowing a save both in terms of thickness and, most of all, mass, respect to a classical homogeneous foam layer.

1 INTRODUCTION

The inclusion of vibroacoustic treatments at early stage of product development, through the use of porous media with periodic inclusions, is a powerful strategy for the achievement of lightweight sound packages and represents a convenient solution for manufacturing aspects.

Indeed, although porous materials are commonly used for vibroacoustic applications, they suffer from a lack of absorption at low frequencies compared to their efficiency at higher ones; this difficulty is usually overcome by multi-layering [1]. However, while reducing the

impedance mismatch at the air-material interface, the efficiency of such devices relies on the allowable thickness [2].

A more efficient way to enhance the low frequency performances of sound packages consists in embedding periodic inclusions in a porous layer [3] in order to create wave interferences or resonance effects that may play a positive role in the dynamics of the system.

The classical approach, known as Floquet-Bloch (F-B) theory, provides a strategy to analyze the behavior of systems with a periodic structure.

In layered systems, due to the heterogeneity of the relevant elastic properties or to particular geometric features, or to both, only certain wave modes can physically propagate inside the structure. Each of these modes can be identified by a determined (generally nonlinear) function relating the time frequency and the spatial frequency (or wave number). These relationships are called dispersion curves and they summarize all the dynamic behavior of the system [4]. Therefore, dispersion curves offer a better perspective to explain the wave field behavior inside bodies.

For instance, the Helmholtz equation is a known example of equation describing the spatial behavior: there, the physical periodic structure of the studied object translates into spatial periodicity of its coefficients. Therefore, the F-B theory can be applied to obtain the dispersive properties of different mechanical periodic systems, reducing the problem to the calculations performed in the so-called unit cell under to certain specific boundary conditions derived from the F-B theory itself [5].

In order to develop efficient numerical techniques to handle the problem, the shift cell operator technique is presented. It allows the description of the propagation of all existing waves from the description of the unit cell through the resolution of a quadratic eigenvalue problem, in which the phase shift of the boundary conditions related to wave propagation is integrated into the partial derivative operator; consequently, the periodicity is included in the overall behavior of the structure, while continuity conditions are imposed at the edges of the unit cell. This is done through a $k(\omega)$ (wave number as a function of the angular frequency) method, which allows computing dispersion curves for frequency-dependent problems; instead of using the classical $\omega(k)$ (angular frequency as a function of wave number) that leads to non-linear eigenvalue problems.

Similar techniques, which use a modified F-B approach in order to handle a $k(\omega)$ problem, can be found in literature ([6]–[8]). The main reason why the shift cell method differs from them is that it consists in a reformulation of classical F-B conditions, in which the phase shift of the boundary conditions related to wave propagation is integrated into the partial derivative operator; consequently, the periodicity is included in the overall behavior of the structure, while continuity conditions are imposed at the edges of the unit cell. This technique has been successfully applied for describing the mechanical behavior of periodic structures embedding visco-elastic materials ([9], [10]) or piezoelectric materials [11]. Here it is proposed an extension to equivalent fluid models: this makes possible to overcome the limits of existing approaches by a more specific design of the system, through a process of optimization and testing of different inclusions, in order to obtain a device whose frequency efficiency outperforms existing designs.

The behavior of the porous materials is described by Johnson-Champoux-Allard (JCA) model ([12], [13]) in the following sections, but one can identically use any other equivalent fluid model ([14]–[16]).

2 SHIFT CELL OPERATOR TECHNIQUE

In this paper, a periodic arrangement of porous materials is considered. For a more detailed discussion, one can refer to [17]. The behavior of each material is described by an equivalent fluid model in the frequency domain, i.e.:

$$\rho \frac{\omega^2}{K} p + \Delta p = 0, \tag{1}$$

where $p = p(\boldsymbol{x}, \omega)$ is the acoustic pressure, $\boldsymbol{x} = (x, y, z)$ is the coordinate vector, ω is the angular frequency, $\rho = \rho(\boldsymbol{x}, \omega)$ is the equivalent fluid density and $K = K(\boldsymbol{x}, \omega)$ is the bulk modulus [18]. The periodicity is described by $\rho(\boldsymbol{x} + \boldsymbol{rn}) = \rho(\boldsymbol{x})$ and $K(\boldsymbol{x} + \boldsymbol{rn}) = K(\boldsymbol{x})$, $\forall \boldsymbol{x} \in \Omega$, where $\boldsymbol{n}$ is a vector of integers normal to the face considered, $\boldsymbol{r} = (\boldsymbol{r_1}, \boldsymbol{r_2}, \boldsymbol{r_3})$ is a matrix containing the three vectors defining the cell periodicity directions and lengths, and Ω is the domain of interest.

For the purpose of the shift cell technique development, considering Eq. 1 and applying the Bloch theorem such as $p(\boldsymbol{x}, \omega) = p(\boldsymbol{x}) e^{j\boldsymbol{kx}}$, where $\boldsymbol{k}$, for a 3D application, is

$$\boldsymbol{k} = k \begin{pmatrix} cos\theta cos\phi \\ cos\theta sin\phi \\ sin\theta \end{pmatrix} \tag{2}$$

one can obtain

$$\boldsymbol{\rho} \frac{\boldsymbol{\omega^2}}{\boldsymbol{K}} \boldsymbol{p} + (\boldsymbol{\nabla} + \boldsymbol{jk})^{\boldsymbol{T}} (\boldsymbol{\nabla} + \boldsymbol{jk}) \boldsymbol{p} = \boldsymbol{0}. \tag{3}$$

$p(x)$ being periodic, the Dirichlet boundary conditions imply $p(L) = p(0)$.

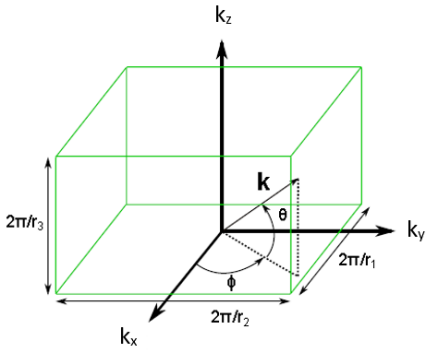

Figure 1: Reciprocal lattice vector in a 3D unitary cell.

2.1. Weak formulation

The aim of this section is the development of the weak formulation of the problem, in order to obtain a matrix equation that fully describes what happens inside a periodic unit cell of equivalent fluid. A weak formulation of Eq. (3) consists in finding p such that $\forall \tilde{p}$, which obeys to the periodic boundary conditions, one has:

$$\begin{aligned} \boldsymbol{\omega^2} \int_\Omega \frac{\boldsymbol{1}}{\boldsymbol{K}} \tilde{\boldsymbol{p}} \boldsymbol{p}\, d\Omega + \int_\Omega \frac{\boldsymbol{1}}{\boldsymbol{\rho}} \tilde{\boldsymbol{p}} \boldsymbol{\nabla^T} \boldsymbol{\nabla p}\, d\Omega + \boldsymbol{jk} \int_\Omega \frac{\boldsymbol{1}}{\boldsymbol{\rho}} \tilde{\boldsymbol{p}} \boldsymbol{\nabla^T p}\, d\Omega + \\ + \boldsymbol{jk^T} \int_\Omega \frac{\boldsymbol{1}}{\boldsymbol{\rho}} \tilde{\boldsymbol{p}} \boldsymbol{\nabla p}\, d\Omega - \boldsymbol{k^T k} \int_\Omega \frac{\boldsymbol{1}}{\boldsymbol{\rho}} \tilde{\boldsymbol{p}} \boldsymbol{p}\, d\Omega = \boldsymbol{0}. \end{aligned} \tag{4}$$

After several passages, considering that $\boldsymbol{\varphi}$ is the eigenvector, the equation can be written in its matrix form

$$(\boldsymbol{K} + \boldsymbol{jkL} + \boldsymbol{k^2 H} - \boldsymbol{\omega^2 M}) \boldsymbol{\varphi} = \boldsymbol{0} \tag{5}$$

with the following matrices:

- $\boldsymbol{K} \propto \int_{\Omega} \frac{1}{\rho} \nabla\tilde{p}\nabla p \, d\Omega$;
- $\boldsymbol{L} \propto \int_{\Omega} \frac{1}{\rho} (\nabla\tilde{p} p - \tilde{p}\nabla p) \, d\Omega$;
- $\boldsymbol{H} \propto \int_{\Omega} \frac{1}{\rho} \tilde{p} p \, d\Omega$;
- $\boldsymbol{M} \propto \int_{\Omega} \frac{1}{K} \tilde{p} p \, d\Omega$.

Here, $\boldsymbol{M}$ and $\boldsymbol{K}$ are respectively the standard symmetric definite mass and symmetric semi-definite stiffness matrices, $\boldsymbol{L}$ is a skew-symmetric matrix and $\boldsymbol{H}$ is a symmetric semi-definite positive matrix. In this formulation, all matrices are frequency dependent.

3 NON-RIGID INCLUSIONS NUMERICAL TEST CAMPAIGN

Herein, all results are related to a 3D unit cell constituted by a cube with side equal to 2 cm (homogeneous case) and with a 0.5 cm radius cylindrical inclusion (cases with inclusion).

The analyses are carried out in the frequency range 0–17000 Hz. It is well known that the parameters of the equivalent fluid models can have a strong impact on the performances of the acoustic device [19], hence they should be determined in a confident way.

In the current case, the characteristics of the materials called “Melamine” and “Black PU” are experimentally determined, while those of the materials called “P1” and “M10” are taken from the work performed by Doutres et al. [20] and those related to “Melamine 173” and “P60” from a paper by Deckers et al. [21]. Except for the “Melamine” and “Melamine 173” materials, all the others are polyurethane foams. While dispersion curves are computed for an infinite repetition of unit cells, absorption coefficient and transmission loss are calculated for a finite repetition of five unit cells, using the same domain and boundary conditions of the infinite periodic system. This, in a first approximation, allows comparing the dispersion relations and the acoustical characteristics of the equivalent finite medium. Indeed, it has been noted that a further increasing in the number of repeated cells would lead to a change in the mean value of absorption coefficient and transmission loss respectively below 2% and 20% compared to the usage of a repetition of five unit cells.

The general definition of the sound absorption coefficient is the fraction of incident energy propagating into a sample material versus the energy propagating out. A part of the incident energy will be absorbed into the sample material, or rather dissipated inside it. The absorption coefficient α can be computed starting from the reflection coefficient R as

$$\alpha = 1 - |R|^2, \tag{16}$$

where R depends on the surface impedance Z_s. The surface impedance of the material is often presented in real and imaginary terms respectively; the real part describes the energy losses whereas the imaginary part describes the phase changes caused by the material [22]:

$$Z_s = \frac{p(L)}{V(L)} = Z_0 \frac{1+R}{1-R}. \tag{6}$$

This technique is only valid for plane waves impinging upon homogeneous media, and just at low frequencies for non-homogeneous ones. In a more general way, that is always correct, the absorption coefficient can be computed as [23]

$$\alpha = \frac{\Pi_{dissipated}}{\Pi_{incident}} \tag{7}$$

where

$$\Pi_{dissipated} = \Pi_{thermal} + \Pi_{viscous} \tag{8}$$

The terms can be expressed as [23]

$$\Pi_{incident} = \frac{S|p_{inc}|^2}{2\rho_0 c_0}, \tag{9}$$

$$\Pi_{thermal} = \frac{1}{2}\Im\left(-\omega \int_{\Omega_p} \frac{\phi^2}{K} p p^* d\Omega\right), \tag{10}$$

$$\Pi_{viscous} = \frac{1}{2}\Im\left(\int_{\Omega_p} \frac{\phi^2}{\omega \tilde{\rho}_{22}} \underline{\nabla} p . \underline{\nabla} p^* d\Omega\right), \tag{11}$$

where

- $S =$ surface interested by incident pressure;
- $p_{inc} =$ amplitude of the excitation mode (incident pressure);
- $\rho_0 =$ density of the interstitial fluid (air);
- $c_0 =$ sound speed in the interstitial fluid (air);
- $\Omega =$ poro-elastic volume;
- $p^* = conj(p)$;
- $\underline{\nabla}\ operator =$ gradient.

The transmission loss is numerically computed as

$$TL = 10\ log_{10} \frac{\Pi_{incident}}{\Pi_{transmitted}} \tag{12}$$

where $\Pi_{incident}$ and $\Pi_{transmitted}$ represent the incident and transmitted power, respectively.

Table 1: Non-acoustic parameters of the foams used for the numerical test campaign.

	Porosity	**Tortuosity**	**Resistivity [Pa*s/m^2]**	**Viscous characteristic length [mm]**	**Thermal characteristic length [mm]**
Melamine	0.99	1.02	8430	0.138	0.154
P1	0.956	1.06	3490	0.187	0.250
Black PU	0.96	1.075	5815	0.102	0.269
M10	0.982	1.25	3670	0.240	0.310
Mel. 173	0.98	1.01	9500	0.166	0.249
P60	0.98	1.17	3750	0.110	0.742

These values are obtained using an implementation of the plane wave forced response of the periodic cell accounting for fluid loading [24]. For a plane wave configuration, the value computed through Eq. (12) for homogeneous flat configurations is equivalent to the one obtained with the Transfer Matrix Method [1]:

$$TL = 10\ log\left(\frac{1}{4}\left|T_{11} + \frac{T_{12}}{\rho_0 c_0} + \rho_0 c_0 T_{21} + T_{22}\right|^2\right), \tag{13}$$

$$\text{with } \begin{bmatrix} T_{11} & T_{12} \\ T_{21} & T_{22} \end{bmatrix} = \begin{bmatrix} cos(kd) & j\,sin(kd)\,Z_0 \\ \frac{j\,sin(kd)}{Z_0} & cos(kd) \end{bmatrix}. \tag{14}$$

3.1. Results

The JCA-modeled 3D unit cell that is described in the previous sections can be tested with some perfectly rigid and non-rigid inclusions. In particular, 48 setups are discussed here (Table 2), whose fundamental parameters are reported in Table 1.

Table 2: Combinations of foams and inclusions used for the numerical test campaign.

Configuration	Foam	Inclusion	Configuration	Foam	Inclusion
1	Melamine	none	25	M10	none
2		rigid	26		rigid
3		air	27		air
4		PU 1	28		PU 1
5		PU black	29		Melamine
6		M10	30		PU black
7		Mel. 173	31		Mel. 173
8		PU 60	32		PU 60
9	P1	none	33	Melamine 173	none
10		rigid	34		rigid
11		air	35		air
12		Melamine	36		PU 1
13		PU black	37		Melamine
14		M10	38		PU black
15		Mel. 173	39		M10
16		PU 60	40		PU 60
17	PU black	none	41	P60	none
18		rigid	42		rigid
19		air	43		air
20		PU 1	44		PU 1
21		Melamine	45		Melamine
22		M10	46		PU black
23		Mel. 173	47		M10
24		PU 60	48		Mel. 173

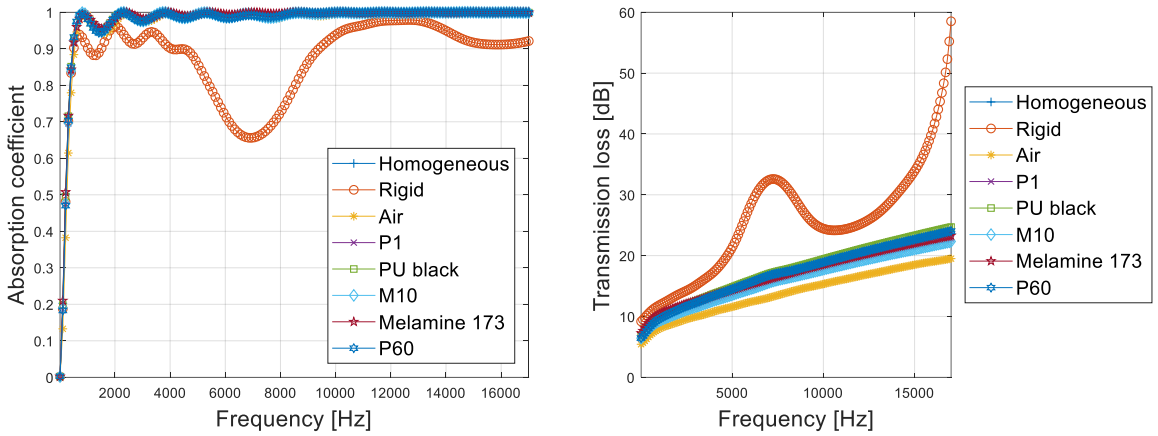

Figure 2: Comparison between absorption coefficient (on the left) and TL (on the right) curves for cases 1-8.

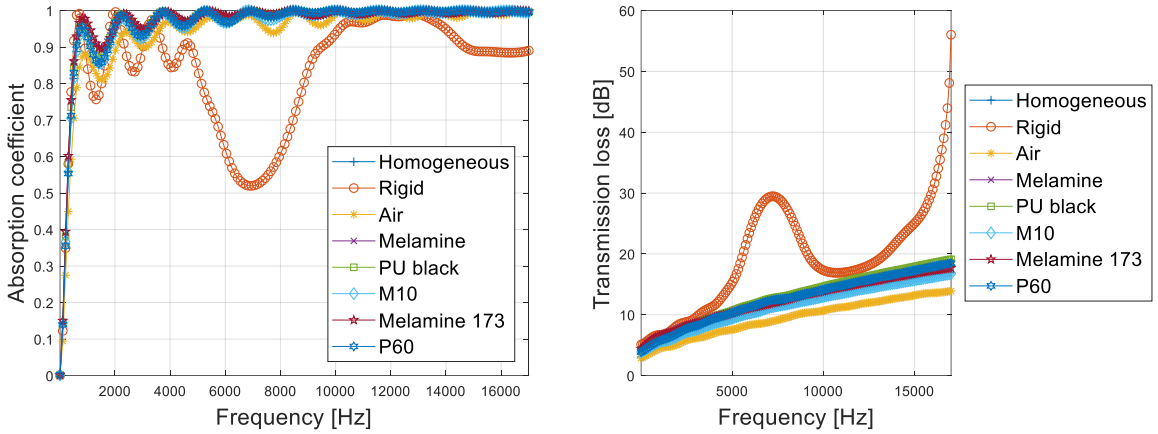

Figure 3: Comparison between absorption coefficient (on the left) and TL (on the right) curves for cases 9-16.

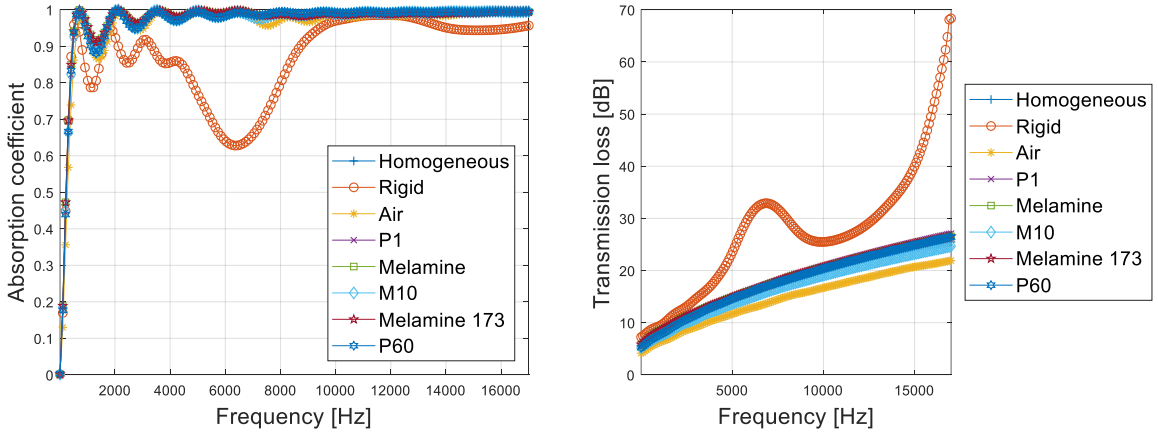

Figure 4: Comparison between absorption coefficient (on the left) and TL (on the right) curves for cases 17-24.

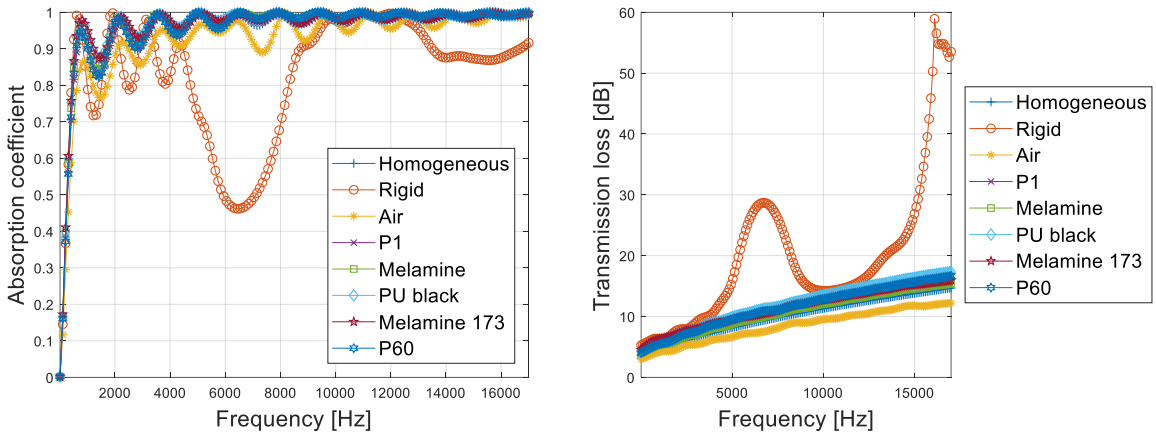

Figure 5: Comparison between absorption coefficient (on the left) and TL (on the right) curves for cases 25-32.

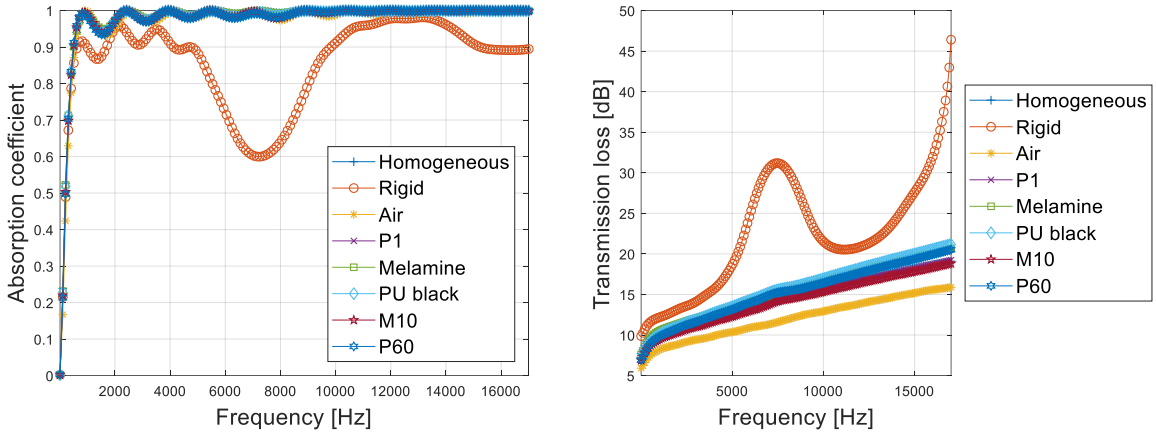

Figure 6: Comparison between absorption coefficient (on the left) and TL (on the right) curves for cases 33-40.

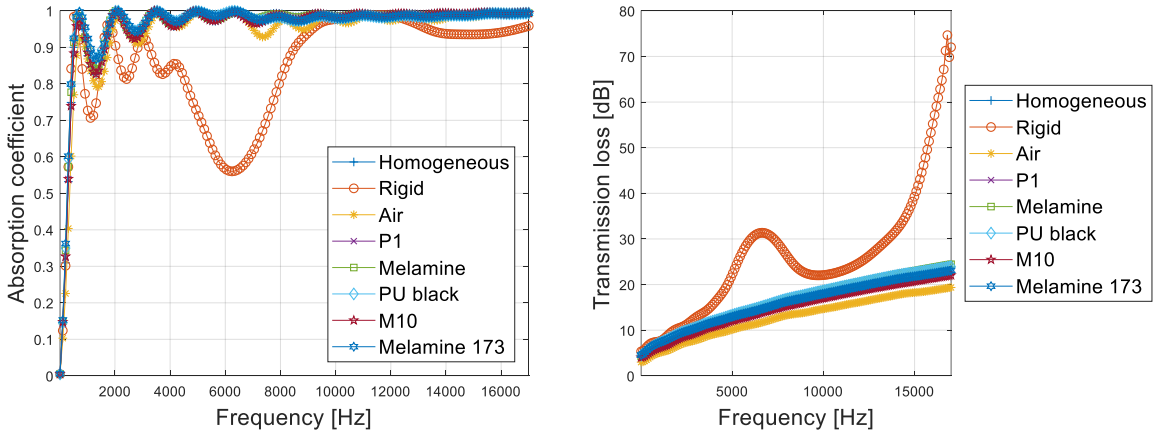

Figure 7: Comparison between absorption coefficient (on the left) and TL (on the right) curves for cases 41-48.

In Figures 2-7, some comparative absorption coefficient and transmission loss plots are shown for each of the 48 cases of study: in particular, each of the six foams is tested using eight different inclusions, according to the combinations reported in Table 2.

It can be noticed that, for what concerns the transmission loss, the effect of the inclusion is not particularly advantageous in these situations: in the case of the air, indeed, there is a drop of performances at all frequencies while, in the case of a foam inclusion, only a slight change of the values can be seen, as well as a very small effect of the periodicity when this is equal to half of the wavelength (around 7000 Hz).

Anyway, some different cases, that may be more interesting from the practical point of view, can be studied by modelling the foam unit cell through the use of the Biot model [25], instead that as an equivalent fluid; doing so, indeed, allows to take into account the elasticity of the skeleton and the entire problem formulation depends not anymore only on the pressure, but on the skeleton displacements too: this means that it should possible to properly write the coupling conditions between the foam and an eventual (non-perfectly rigid) solid inclusion.

4 COMPARISON OF ACOUSTIC PERFORMANCES BETWEEN A HOMOGENEOUS UNIT CELL AND AN UNIT CELL WITH INCLUSION WITH FIXED MASS

In the previous sections, all the comparisons between homogeneous cases and cases with inclusions are made considering unit cells with the same dimensions; in other words, it means that the performances of a layer with periodic inclusions are estimated assuming that is has the same thickness of the related homogeneous one.

One may want also to compare absorption coefficient and transmission loss plots for the case in which the unit cell with inclusion has the same mass (and therefore different dimensions) respect to the homogeneous one. For example, considering an unit cell made of Melamine and with a perfectly rigid inclusion (Configuration 2 of Table 2), when comparing it to the homogeneous case with fixed dimensions, it obviously has a slower mass (75.56% of the homogeneous unit cell value); therefore, in order to perform a comparison with fixed mass respect to the homogeneous case, one should increase each dimension of the unit cell with inclusion of a certain quantity that, for the specific case, is equal to the 7.56%.

At this point, making some considerations based on the results shown in Figures 8 and 9, one may notice that the curve with fixed mass, respect to the one with fixed dimensions, has a performance peak caused by periodicity effect that is shifted at lower frequencies (this is due to the different dimensions between the two cases with inclusion) and also of different amplitude (due to the different mass of the compared unit cells).

Furthermore, in order to obtain the same transmission loss performances in the periodicity peak range (between 6000 and 8000 Hz, for the specific cases considered) by the use of a simple homogeneous layer made of the same foam, one should use a thickness that is around twice the one required for the cases with inclusion, therefore leading to an increment of the mass of about 100%. This clearly point out the advantage of designing foam layer with periodic inclusion patterns in order to improve the performances in a specific range of frequencies, allowing a save both in terms of thickness and, most of all, mass, respect to a classical homogeneous foam layer.

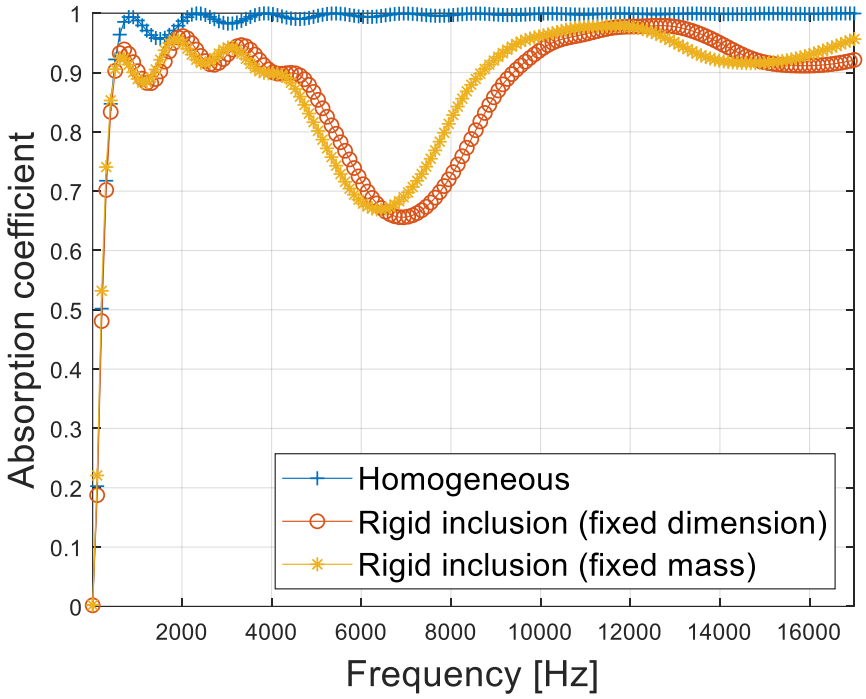

Figure 8: Comparison of absorption coefficient curves between the homogeneous case, the case with inclusion with fixed dimensions and the case with inclusion with fixed mass.

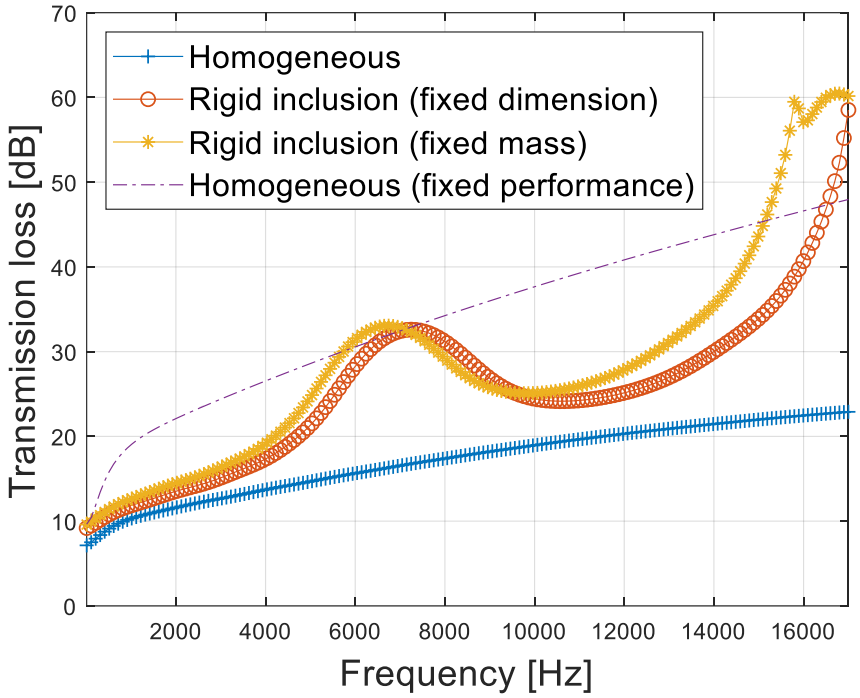

Figure 9: Comparison of transmission loss curves between the homogeneous case, the case with inclusion with fixed dimensions, the case with inclusion with fixed mass and the homogeneous case with fixed performance in the 6000-8000 Hz frequency range.

5 CONCLUSIONS

The shift cell technique has been presented, providing details on its numerical formulation.

Numerical results have been shown, in terms of absorption coefficient and transmission loss curves obtained through a test campaign involving 48 different JCA-modelled melamine and polyurethane foam unit cell configurations.

Furthermore, it has been shown the comparison between absorption coefficient and transmission loss plots for the case in which the unit cell with inclusion has the same mass (and therefore different dimensions) respect to the homogeneous one.

Further developments of the work will include the implementation of the shift cell technique using Biot model, for both 2D and 3D geometries, as well as the design and experimental tests of a specific unit cell configuration, chosen accordingly to an optimization process that will involve geometry, foam and inclusion material.

ACKNOLEDGEMENTS

This project has received funding from the European Union's Horizon 2020 research and innovation program under the Marie Skłodowska-Curie grant agreement No. 675441.

REFERENCES

[1] J. F. Allard and N. Atalla, *Propagation of Sound in Porous Media: Modelling Sound Absorbing Materials*, 2nd ed. Wiley, 2009.

[2] T. Weisser *et al.*, "Acoustic behavior of a rigidly backed poroelastic layer with periodic resonant inclusions by a multiple scattering approach," *J. Acoust. Soc. Am.*, vol. 139, no. 2, pp. 617–629, 2016.

[3] J.-P. Groby, a Wirgin, L. De Ryck, W. Lauriks, R. P. Gilbert, and Y. S. Xu, "Acoustic response of a rigid-frame porous medium plate with a periodic set of inclusions.," *J. Acoust. Soc. Am.*, vol. 126, no. 2, pp. 685–693, 2009.

[4] Floquet and Gaston, "Sur les équations différentielles linéaires à coefficients périodiques," *Ann. Sci. l'École Norm. Supérieure*, vol. 12, no. Série 2, pp. 47–88, 1883.

[5] P. G. García and J.-P. Fernández-Álvarez, "Floquet-Bloch Theory and Its Application to the Dispersion Curves of Nonperiodic Layered Systems," *Math. Probl. Eng. Math. Probl. Eng.*, vol. 2015, 2015.

[6] M. A. Lewińska, J. A. W. van Dommelen, V. G. Kouznetsova, and M. G. D. Geers, "Towards acoustic metafoams: the enhanced performance of a poroelastic material with local resonators," *J. Mech. Phys. Solids*, 2018.

[7] A. O. Krushynska, V. G. Kouznetsova, and M. G. D. D. Geers, "Visco-elastic effects on wave dispersion in three-phase acoustic metamaterials," *J. Mech. Phys. Solids*, vol. 96, pp. 29–47, 2016.

[8] Y. F. Wang, Y. S. Wang, and V. Laude, "Wave propagation in two-dimensional viscoelastic metamaterials," *Phys. Rev. B - Condens. Matter Mater. Phys.*, vol. 92, no. 10, pp. 1–14, 2015.

[9] M. Collet, M. Ouisse, M. Ruzzene, and M. N. Ichchou, "Floquet-Bloch decomposition for the computation of dispersion of two-dimensional periodic, damped mechanical systems," *Int. J. Solids Struct.*, vol. 48, no. 20, pp. 2837–2848, 2011.

[10] K. Billon *et al.*, "Design and experimental validation of a temperature-driven adaptive

phononic crystal slab," *Smart Mater. Struct.*, vol. 28, no. 3, pp. 1–23, 2019.
[11] M. Collet, M. Ouisse, and F. Tateo, "Adaptive metacomposites for vibroacoustic control applications," *IEEE Sens. J.*, vol. 14, no. 7, pp. 2145–2152, 2014.
[12] D. L. Johnson, J. Koplik, and R. Dashen, "Theory of dynamic permeability and tortuosity in fluid-saturated porous media," *J. Fluid Mech.*, vol. 176, no. 1, p. 379, 1987.
[13] Y. Champoux and J. F. Allard, "Dynamic tortuosity and bulk modulus in air-saturated porous media," *J. Appl. Phys.*, vol. 70, no. 4, pp. 1975–1979, 1991.
[14] M. E. Delany and E. N. Bazley, "Acoustical properties o f fibrous absorbent materials," *Appl. Acoust.*, no. 3, 1969.
[15] Y. Miki, "Acoustical properties of porous materials-Modifications of Delany-Bazley models," *J. Acoust. Soc. Jpn.(E)*, vol. 11, no. 1, pp. 19–24, 1990.
[16] D. Lafarge, P. Lemarinier, J. F. Allard, and V. Tarnow, "Dynamic compressibility of air in porous structures at audible frequencies," *J. Acoust. Soc. Am.*, vol. 102, no. 4, pp. 1995–2006, 1997.
[17] D. Magliacano *et al.*, "Computation of dispersion diagrams for periodic porous materials modeled as equivalent fluids," *J. Sound Vib.*, 2018.
[18] A. Bensoussan, J. L. Lions, and G. Papanicolaou, "Asymptotic Analysis of Periodic Structures," *Stud. Math. its Appl.*, vol. 5, no. Elsevier, 1978.
[19] M. Ouisse, M. Ichchou, S. Chedly, and M. Collet, "On the sensitivity analysis of porous material models," *J. Sound Vib.*, vol. 331, no. 24, pp. 5292–5308, 2012.
[20] O. Doutres, M. Ouisse, N. Atalla, and M. Ichchou, "Impact of the irregular microgeometry of polyurethane foam on the macroscopic acoustic behavior predicted by a unit-cell model," *J. Acoust. Soc. Am.*, vol. 136, no. 4, pp. 1666–1681, 2014.
[21] E. Deckers, S. Jonckheere, and D. Vandepitte, "Modelling Techniques for Vibro-Acoustic Dynamics of Poroelastic Materials," pp. 183–236, 2015.
[22] M. Wolkesson, "Evaluation of impedance tube methods - A two microphone in-situ method for road surfaces and the three microphone transfer function method for porous materials," p. 69, 2013.
[23] F. Sgard, F. Castel, and N. Atalla, "Use of a hybrid adaptive finite element/modal approach to assess the sound absorption of porous materials with meso-heterogeneities," *Appl. Acoust.*, vol. 72, no. 4, pp. 157–168, 2011.
[24] N. Atalla, *NOVAFEM User's guide*. Sherbrooke (QC, Canada): Université de Sherbrooke, 2017.
[25] M. a Biot, "Mechanics of Deformation," *J. Appl. Physiscs*, vol. 33, no. 4, pp. 1482–1498, 1962.